[79] M. Imai, M. Suzaki, and T. Matsumoto, "Some consideration on a lens-like medium with aberrations," *J. Inst. Electron. Commun. Eng. Jap.*, vol. 52-B, p. 491, Sept. 1969.
[80] S. Sawa and N. Kumagai, "Analysis of the optical beam waveguide consisting of tapered lens-like medium and its applications," *J. Inst. Electron. Commun. Eng. Jap.*, vol. 54-B, pp. 190–197, Apr. 1971.
[81] Y. Suematsu and K. Furuya, "Vector wave solution of light beam propagating along lens-like medium," *Trans. Inst. Electron. Commun. Eng. Jap.*, vol. 54-B, pp. 325–333, June 1971.
[82] S. Uehara, Y. Yamauchi, and T. Isawa, "Optical intensity modulator with waveguide structure," *Appl. Phys. Lett.*, vol. 24, Jan. 1, 1974.
[83] Y. Izutsu, S. Noda, F. Abe, and T. Sueta, "Modulation of 10.6 μm wave by GaAs slab plate," in *Kansai Conv. Rec., Inst. Electron. Commun. Eng. Jap.* (1973), Paper G10-22.
[84] S. Takada, M. Ohnishi, H. Hayakawa, and N. Mikoshiba, "Optical waveguides of single-crystal $LiNbO_3$ film deposited by r-f sputtering method," *Appl. Phys. Lett.*, May 15, 1974, to be published.

Heterostructure Injection Lasers

MORTON B. PANISH

(*Invited Paper*)

***Abstract*—The utilization of the nearly ideal heterojunction that can be achieved between GaAs and $Al_xGa_{1-x}As$ to confine both light and electrical carriers has lead to the evolution of several new classes as injection lasers with very low room-temperature current-density thresholds for lasing ($\lesssim$1000 A/cm²), and structures whose operation can be more readily understood than the earlier homostructure lasers. These are as follows: the single-heterostructure (SH) laser which utilizes one heterojunction to confine light and carriers on one side of the structure; the double-heterostructure (DH) laser in which both carriers and light are confined to the same region; and the separate-confinement-heterostructure (SCH) laser in which the carriers are separately confined to a narrow region within the optical cavity. A state-of-the-art description of these lasers and some of the mode structures encountered in their operation is presented. Recent work is described which permits the growth of low-strain heterostructures with heterojunctions between GaAs and $Al_xGa_{1-x}As_{1-y}P_y$ strain reduction from mismatch and bonding of contacts has resulted in lasers which, while maintaining very low room-temperature current thresholds, also have very long lifetimes (>10⁵ h) for continuous operation.**

INTRODUCTION

ONE of the important candidates being considered as the signal generator for optical-communications systems is the heterostructure injection laser. Lasing action by the stimulated recombination of carriers injected across a p-n junction was predicted [1], [2] in 1961 and was achieved [3]–[6] in 1962. These early injection lasers were generally rectangular chips of GaAs containing a p-n junction perpendicular to two polished or cleaved ends of the chip. The structure is illustrated in Fig. 1. The polished or cleaved ends are partial mirrors. Light is generated by the injection of electrons into the p region with subsequent radiative recombination of holes and electrons. This recombination occurs in a volume adjacent to the p-n junction and between the two mirrors. The active region between the mirrors is then an optical cavity. Structures such as that illustrated in Fig. 1 are now generally referred to as homostructure lasers because they are made of a single material such as GaAs, and thus contain no heterojunctions. These types of injection lasers typically have very high room-temperature-threshold current densities (~50 000 A/cm²), because little or no control over the thickness of the recombination region can be achieved as the result of unrestricted diffusion of injected carriers and because that region constitutes a very poor waveguide. The band-edge potential diagram, the refractive index, and the optical-field dis-

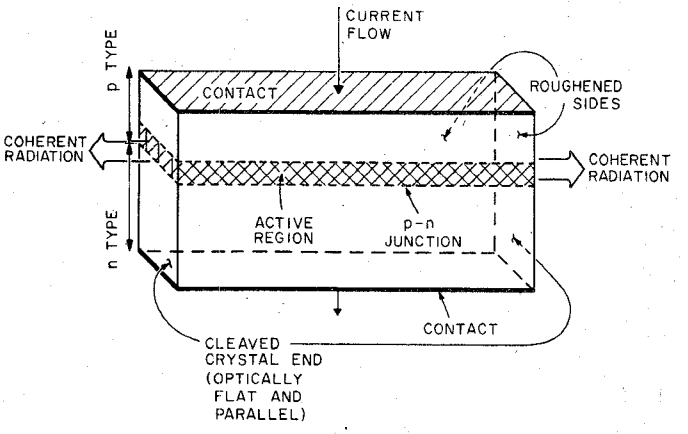

Fig. 1. A homostructure p-n junction laser in the form of a Fabry–Perot cavity. After Panish and Hayashi [21].

Manuscript received March 6, 1974; revised April 25, 1974.
The author is with Bell Laboratories, Murray Hill, N. J. 07974.

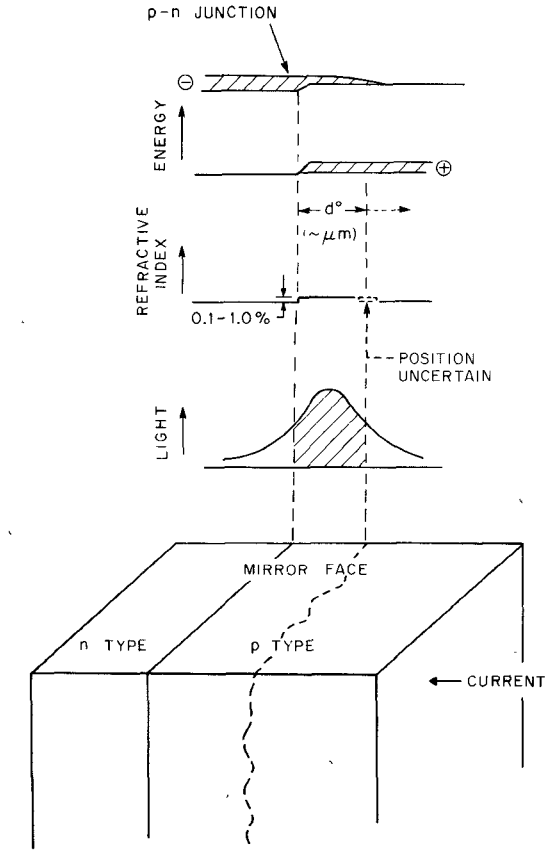

Fig. 2. Schematic representation of the band edges (forward biased), refractive index, and optical-field distribution in diffused homostructure laser diodes. The possibility of uncertainty in the position and regularity of the right boundary of the active region is exaggerated for illustrative purposes. The energy bands are shown with high forward bias and both the n and p regions are degenerately doped. Electrons are injected into the p region but hole injection is negligible. The injected electron population is great enough so that in the region $d°$ the condition that the separation of the quasi-Fermi levels for electrons and holes $F_c - F_v > h\nu$ is satisfied. After Panish and Hayashi [21].

tribution for a homostructure laser are shown schematically in Fig. 2 for a comparison with the more complex structures that will be discussed.

In 1963 Kroemer [7] and Alferov and Kazarinov [8] suggested that the junction laser could be improved by the use of structures with heterojunctions, in which the recombination or active region is bounded by wider band-gap regions. These initial suggestions did not immediately result in injection lasers with lower threshold currents at room temperature [9], [10] because the materials combination suggested at that time, GaAs–$GaAs_xP_{1-x}$, led to the generation of nonradiative traps at lattice-mismatched heterojunctions. In 1967 Rupprecht *et al.* [11] reported the growth by liquid-phase epitaxy (LPE) of layers of $Al_xGa_{1-x}As$ on GaAs. The band gap of $Al_xGa_{1-x}As$ increases with x and is direct to about $x = 0.37$ [12]. Furthermore the replacement of Ga with Al atoms in the lattice has only a very small effect upon the lattice parameter so that heterojunctions between GaAs and $Al_xGa_{1-x}As$ are very nearly lattice matched. It thus appeared that with sufficient control of the layered growth and understanding of the parameters involved, improved junction lasers could be achieved. At about that time, therefore, Alferov [13], [14], Hayashi and Panish [15]–[17], and Kressel [18], all with co-workers, began studies which resulted in injection lasers with reduced room-temperature current thresholds, and eventually lasers capable of operating continuously at room temperature [19], [20].

These lasers, which are designated as heterostructure lasers, fall into three general classes: 1) single-heterostructure (SH) lasers, in which there is only one heterojunction so that light and injected carriers are confined by a heterojunction only at one boundary of the recombination region; 2) double-heterostructure (DH) lasers, in which the carriers and waveguide have the same boundaries on both sides of the recombination region; and 3) separate-confinement heterostructures (SCH), in which the injected carriers are confined to a region within the waveguide. The discussion which follows is a state-of-the-art description of the pertinent physical and chemical properties of GaAs and $Al_xGa_{1-x}As$, of the nature of heterojunctions in the $Al_xGa_{1-x}As$ system, of the properties of several types of heterostructure lasers, and of the degradation of such lasers. A more detailed review is given in [21].

MATERIAL PROPERTIES AND CRYSTAL GROWTH

GaAs and $Al_xGa_{1-x}As$ are semiconductors which crystallize with the zinc-blende lattice structure. The Group III and Group V elements occupy separate sublattices, and thermodynamic studies of $Al_xGa_{1-x}As$ suggest that the Al and Ga are randomly placed on the Group III lattice sites [22], [23]. GaAs is a direct-gap material with a forbidden energy E_g of 1.43 eV at room temperature. The band gap of $Al_xGa_{1-x}As$ increases with x to a transition from a direct to an indirect gap at ~1.92 eV and $x = 0.37$. This is illustrated in the composition-energy diagram of Fig. 3 obtained with data from [12], [24], and [25]. Efficient radiative recombination can readily be achieved in GaAs and in $Al_xGa_{1-x}As$ with compositions in the direct-gap range. Efficient light-emitting diodes have been made with both materials, and minority-carrier diffusion lengths in GaAs have been studied [26]–[28]. These diffusion lengths are long, on the order of several microns for material doped in the 10^{17}–10^{18}-cm^{-3} range. This long diffusion length is an important characteristic because, as will be described later, it is possible to achieve heterostructure lasers with recombination- or active-region widths which are small compared to the diffusion length. Calculations of the optical-field distribution in GaAs–$Al_xGa_{1-x}As$ heterostructure lasers require a detailed knowledge of the refractive index $\bar{n}$ of GaAs and $Al_xGa_{1-x}As$ as a function of wavelength and composition. For GaAs $\bar{n}$ is, in the spectral region of interest, considerably influenced by doping [29]. Detailed new information has recently become available for the refractive index of both GaAs and $Al_xGa_{1-x}As$ [29], [30], and the results have been used in several field calculations which

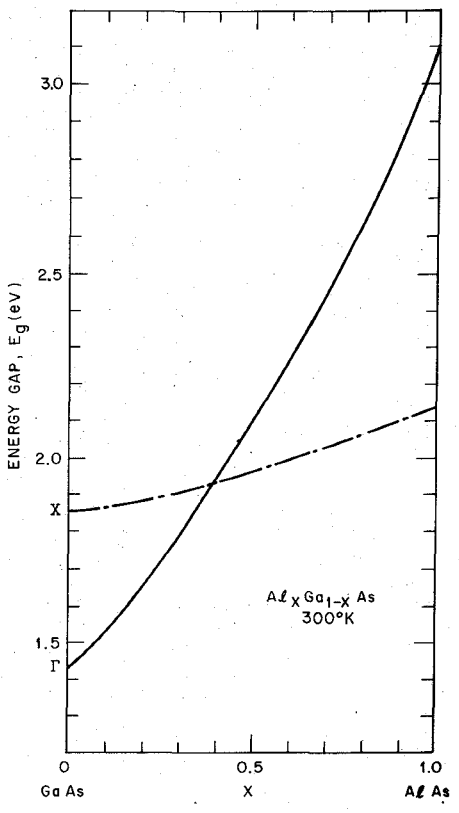

Fig. 3. Direct —— and indirect - — - — band-gap energy of $Al_xGa_{1-x}As$ against composition.

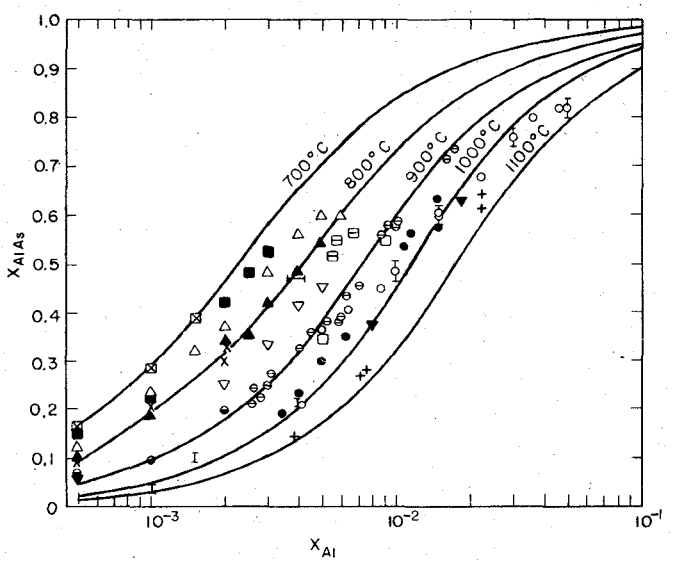

Fig. 5. Solidus isotherms in the Al–Ga–As system. The liquid composition is defined by one elemental composition, x_{Al}, since the liquidus isotherms are defined in Fig. 4. In practice the the liquidus may be considered to be the indicated atom fraction of Al in an Al–Ga solution where it is then saturated with As or GaAs. ⊠, ×, ○, I [34], at 700, 800, 900, and 1000°C, respectively. ⊢, ⊟, ⊖ [33], at 800, 850, and 900°C, ○ [23] at 1000°C, ⊕ [22] at 1000°C. ■ 707°C, △ 756°C, ▲ 802°C, ▽ 852°C, □ 900°C, ● 970°C, ▼ 1020°C, + 1060°C [32]. The solid curves are estimated from the experimental data with a simple solution treatment. After Panish and Hayashi [21].

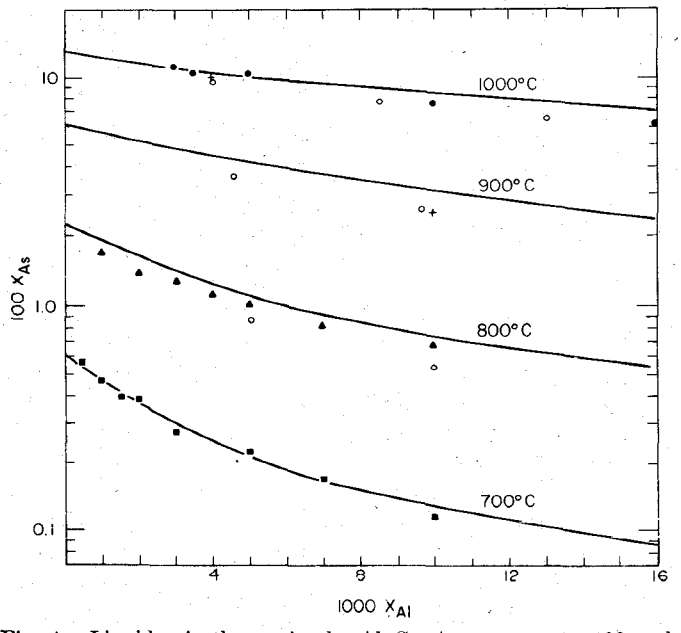

Fig. 4. Liquidus isotherms in the Al–Ga–As system. +: 900 and 1000°C [22]. ○: 800, 900, and 1000°C [23]. ■ 712. ▲ 802. ● 1000°C [32]. The solid curves are estimated from the experimental data with a simple solution treatment. $X_{Ga} + X_{Al} + X_{As} = 1$. After Panish and Hayashi [21].

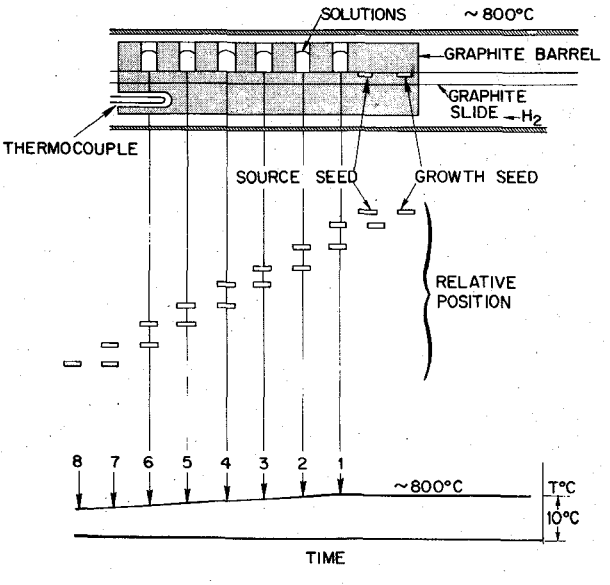

Fig. 6. A recent version of apparatus and procedures used for the growth of DH lasers. The growth boat, the apparatus, and growth and source seed positions relative to solutions and temperature are shown. The procedure results from the work of authors Dawson [71] and Rode [72].

are illustrated in the following discussion of modes and far-field distributions.

At the time of this writing there have been two successful techniques for the preparation of heterostructure wafers. The most frequently used has been LPE, but more recently molecular-beam epitaxy has shown great promise [31]. LPE is a near-equilibrium growth technique in which the successive layers constituting the heterostructure are grown onto a GaAs substrate by successively bringing the substrate into contact with Al–Ga–As or

Ga–As solutions, properly doped, while cooling. It is clear that the composition–temperature relationships for the Al–Ga–As system must be well in hand. A number of phase studies have been done [22], [23], [32]–[34] and the resulting phase diagrams for the liquidus and solidus equilibria at several temperatures are given in Figs. 4 and 5. For lasers, the multilayer growth is generally done near 800°C. The apparatus used recently by this author is shown in Fig. 6. As illustrated, the layers are grown by successively bringing the different solutions into contact with the seed while cooling at 0.05–0.1°C/min. A first seed is generally used to bring the solutions to saturation with respect to arsenic. Solution compositions are chosen from the phase data for the required layer compositions. Dopants are added to the solution.

Molecular-beam epitaxy is a technique based upon the early studies of Arthur [35], which has been further studied and refined by Cho *et al.* [36], [37], for growing multilayers of GaAs and $Al_xGa_{1-x}As$ and which has recently been used to achieve low-threshold DH lasers [31]. The technique consists of impinging controlled beams of Ga, Al, and dopant atoms, and As_2 or As_4 molecules upon a heated substrate. Epitaxy results when the beam contains excess arsenic. This technique is characterized by its potentiality for a very high degree of dimensional control.

THE HETEROJUNCTION IN THE $Al_xGa_{1-x}As$ SYSTEM

The simplest case to discuss is the GaAs–$Al_xGa_{1-x}As$ heterojunction, and the discussion applies also to the more general case of $Al_xGa_{1-x}As$–$Al_gGa_{1-g}As$, in which at least one side of the junction is in the direct-gap composition region. The features of the GaAs–$Al_xGa_{1-x}As$ heterojunction are the wider band gap of $Al_xGa_{1-x}As$, the lack of extensive interface recombination by nonradiative traps, and the fact that the discontinuity in the band-gap energy between GaAs and $Al_xGa_{1-x}As$, while essentially a conduction-band discontinuity when defined in terms of the electron affinity, can be used effectively as a barrier to holes and electrons by adjusting the doping. Schematic diagrams of the band edges for various of the combinations of heterojunctions possible are shown in Fig. 7. A convenient notation which will be used from here on is to use n and p for designating n–GaAs and p–GaAs and N and P to designate n-type $Al_xGa_{1-x}As$ and p-type $Al_xGa_{1-x}As$. For simplicity the Fermi levels of n- and N-type material and of p- and P-type material are taken in Fig. 7 to be at the conduction and valence band edges, respectively. In the lower part of the figure, junctions between materials of different conductivity types are shown at high forward bias so as to permit electron injection (at a p-N heterojunction) or hole injection (at an n-P heterojunction) as shown. At the n-N and N-p heterojunctions the conduction band difference between GaAs and $Al_xGa_{1-x}As$ is expected to cause a discontinuity (shown dotted) in the conduction band. This narrow potential barrier is generally taken to permit passage of

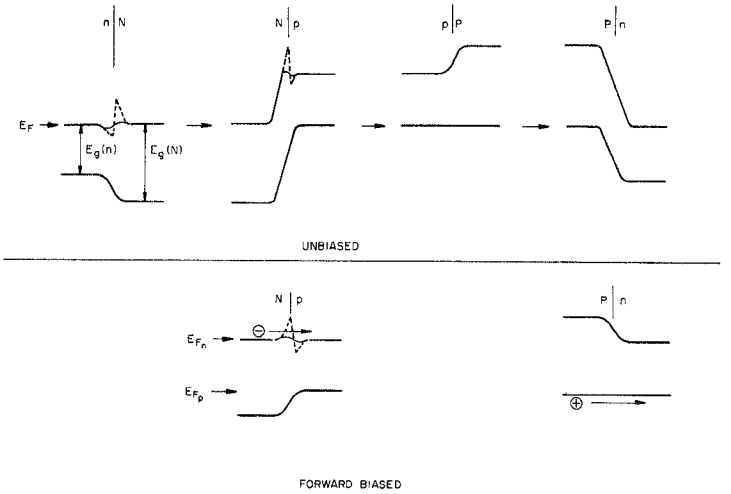

Fig. 7. A schematic drawing of band-edge potential diagrams of n-N, N-p, p-P, and P-n heterojunctions between GaAs and $Al_xGa_{1-x}As$. - - - ungraded junction; —— graded junction. E_F, Fermi level in unbiased case. E_{F_n} and E_{F_p}, Fermi levels in biased case. Fermi levels are taken to coincide with the band edges. E_g shows the forbidden gap.

carriers by tunneling, or to be largely smeared out by composition gradients over relatively short distances [38]. The result of this is, as described for specific structures in the following, that the band-gap difference between GaAs and $Al_xGa_{1-x}As$ is a potential barrier that reflects electrons at p-P and p-N heterojunctions and holes at N-p and N-n heterojunctions. The existence of these potential barriers to minority carriers permits sufficient biasing of the junction devices so that the injected carrier density in the active layer becomes greater than the equilibrium majority carrier density in the emitting layer. Alferov [39] has called this ability to achieve such high injected carrier densities "superinjection."

HETEROSTRUCTURE LASERS

A. Single Heterostructure Lasers

The first reduction of room-temperature current thresholds Jth (300 K) of injection lasers was achieved with a structure which is illustrated in Fig. 8 and is designated in the notation described previously as a n-p-P structure, the so-called single heterostructure. In this structure the p-n junction is located a short distance (about 2 μm usually) from the p-P heterojunction. Under forward bias, electrons are injected across the n-p junction but are then confined by the potential barrier at the p-P junction. Improvement in the establishment of a well-defined active region and optical waveguide over that achieved with the homostructure laser can be qualitatively seen by comparison of Figs. 2 and 8. A plot of Jth (300 K) and Jth (80 K) as a function of the thickness d of the active region is given in Fig. 9. It can be seen that over a considerable range Jth decreases with d. This suggests that the injected electrons are indeed confined by the p-P barrier so that Jth behaves as expected, i.e., decreases with the volume of the active region. At sufficiently small d, however, Jth increases with decreasing d. This can

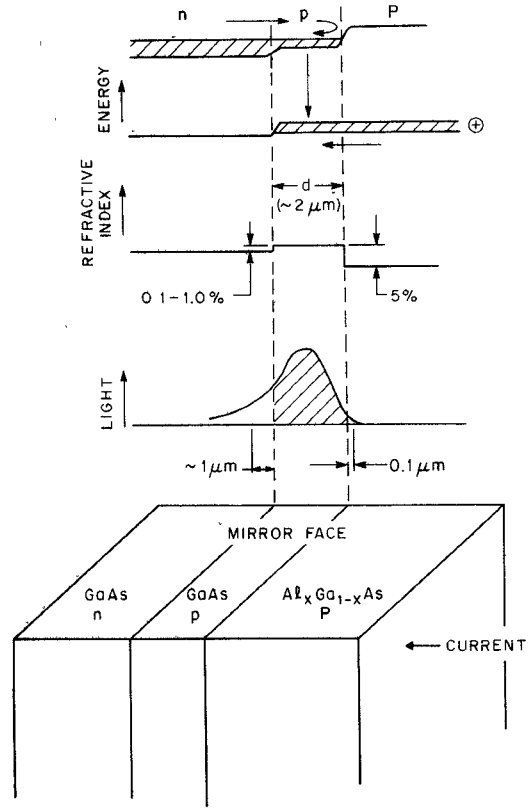

Fig. 8. Band structure, refractive index, optical power distribution, and physical structure of an SH laser. After Panish and Hayashi [21].

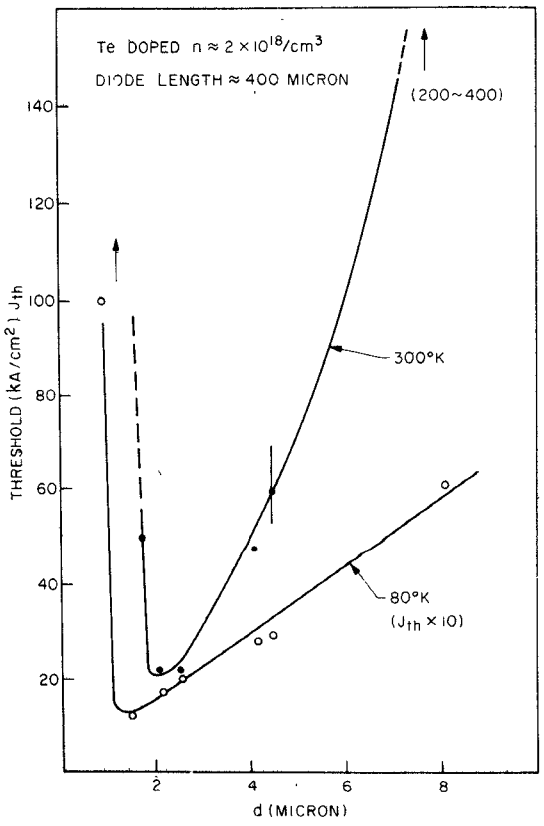

Fig. 9. Jth as a function of d for uncoated (~400 μm-long) Fabry–Perot SH diodes at 300 and 80 K. All diodes used for this plot were made on 2 × 10^{18} n/cm^3 Te-doped GaAs. After Hayashi and Panish [17].

result from hole injection when the structure with smaller d must have higher forward bias to reach the lasing electron density because of the greater spread of the optical field out of the active region, and it can also be due to the failure of the optical-field confinement as a result of increasing asymmetry of the structure with decreasing d. With the SH laser, Jth (300 K) in the range of 8000–15 000 A/cm^2 is readily achieved [15], [18]. These lasers are generally operated with a short duty-cycle current pulse (typically on the order of 0.1 μs at 100–1000 Hz) and have not been run continuously at room temperature. Some typical SH-laser parameters are given in Tables I and II.

B. Double Heterostructure Lasers

The DH laser of GaAs–$Al_xGa_{1-x}As$ is presently the most important heterostructure-laser candidate being developed for use in optical-communications systems. It was the first junction laser capable of continuous operation at room temperature [19], [20] (and even well above [40]), and for which long-lived versions are available [41]. Its layer structure is N-p-P or N-n-P as illustrated in Fig. 10. Minority carriers are effectively confined to the narrow-gap region, the boundaries of which also correspond to the waveguide The properties of the DH are found to be primarily dependent upon the dimensions of the structure and the composition of the wide-gap regions. At active-region doping levels less than ~10^{18} cm^{-3} the DH-laser properties are not strongly dependent upon the doping element or level.

With this structure Jth (300 K) is clearly proportional to the volume of the active region for d greater than about 0.5 μm as is shown for the data for Jth (300 K) against d for a particularly uniform set of diodes in Fig. 11. The thresholds are much lower than those which can be achieved with SH lasers and are achieved at narrower active-region widths. These reduced thresholds result not only from a smaller active volume, reduced loss, and better coupling of the optical field to the active region than in the SH or homostructure laser, but also from greater superinjection. This permits the electron quasi-Fermi level in a p-type active region, for example, to be pushed further into the conduction band with the result that the quasi-Fermi level comes closer to the maximum in the electron distribution in the conduction band [21]. Some typical parameters for DH lasers are given in Tables I and II.

C. Filaments and Modes

One of the difficult problems which must be dealt with in studies of injection lasers is their tendency towards multimode and filamentary operation. A lasing filament is a relatively narrow region of an injection laser which, presumably because of small inhomogenieties in the structure, begins to lase while surrounding regions are still below threshold. These filaments tend to be unstable and cause noise, and with increasing current above threshold multifilament operation is possible in a sufficiently

TABLE I
TYPICAL 300 K HETEROSTRUCTURE LASER PARAMETERS[a]

	SH	Ref	DH	Ref	SCH	Ref
J_{th}/(A/cm^2)	8000-15,000	17,18	~1000-6000[c]		575-2500	55,69
J_{th}/d/(A/cm^2 μ	~6000-10,000[b]	17	~4000-5000			
gain/(cm/KA)	3-6	17,18				
Loss/(cm^{-1})	20-40	17,18	~10[d]	67	9-17[d]	55
g = J^m,m	1	17,66	~2.8	68	~3	55
efficiency($^{\text{differential}}_{\text{external}}$)	20-50%	17,56	40-50%	68	40-60%	55
efficiency ($^{\text{total}}_{\text{external}}$)	~10%	17,56			~40%[e]	55

[a] For pulsed lasers with Fabry–Perot cavities 0.4–1.0 mm long.
[b] $d \sim 1.5$–3.0 μm.
[c] $d \sim 0.2$–1.5 μm.
[d] For active regions doped less than about 10^{18} carriers/cm^3.
[e] At four times Jth (300 K), one typical unit tested. Fundamental transverse mode.
[f] Symmetrical SCH. Data for LOC-type structures are given in [52] and [73].

TABLE II
POWER AND CURRENT FOR SEVERAL TYPICAL HETEROSTRUCTURE LASERS

	External Pulsed Peak Power Watts	at	Pulsed Peak Current I/AMPS	External CW Power Watts	at	CW Current I/AMPS
SH	13 (Ref 56)		24	No CW SH lasers		
DH	6[a] (Ref 56)		10	≈ 0.01 (stripe[b])		0.1-0.2
				0.2[a] (broad area[c] Ref 70)		1-2
SCH	3-4[a] (Ref 55)		19	No data available		

[a] Maximum measured.
[b] Typical stripe-laser dimensions are 10 × 400 μm.
[c] Typical broad-area-laser dimensions are 100 × 400 μm.

wide structure. The problem is alleviated by passing current through a narrow-stripe laser rather than a wide area. This stripe which can be defined by a stripe contact [42], proton bombardment [40], doping profile control [43], or a stripe mesa structure [44] is usually about 10 μm wide and can accommodate only a single filament. These various approaches to filament control are illustrated in Fig. 12.

The stripe-geometry lasers, when uniform enough, exhibit mode structures parallel to the junction plane, with the order of the mode increasing with the width of the stripe [45]. These parallel modes have also been observed with stripe-geometry lasers employing the doping profile control [43]. The fundamental mode is obtained for stripe widths of about 12 μm or less so that the criteria for fundamental parallel-mode operation and single-filament operation are the same. Mode confinement parallel to the junction is related to the presence of gain within the stripe confines [46], [47].

In the DH laser the transverse modes perpendicular to the junction plane are generally TE rather than TM because TE modes have a larger reflectivity at the cavity mirror and therefore a lower cavity loss and a lower threshold current density. For the same reason higher order TE modes are preferred because they have a larger angle of incidence and thus lower mirror loss than lower order modes. Mode selection results, however, from a balance between the decrease of mirror loss with increasing mode order and an increase of loss within the volume of the device with increasing order since the higher order modes penetrate farther into the inactive regions which bound the active region. It is usually desirable to maintain the lowest order (fundamental) mode in a practical device. Fortunately, the requirements for fundamental-mode operation and low threshold coincide because of the need for a thin active region in both cases. In structures with sufficiently thick active regions the threshold of a higher order mode can become comparable to that of the fundamental mode so that multimode operation can occur. The elimination of this kind of higher order and multimode operation requires that the gain profile be controlled in such a way as to favor one mode. The SCH

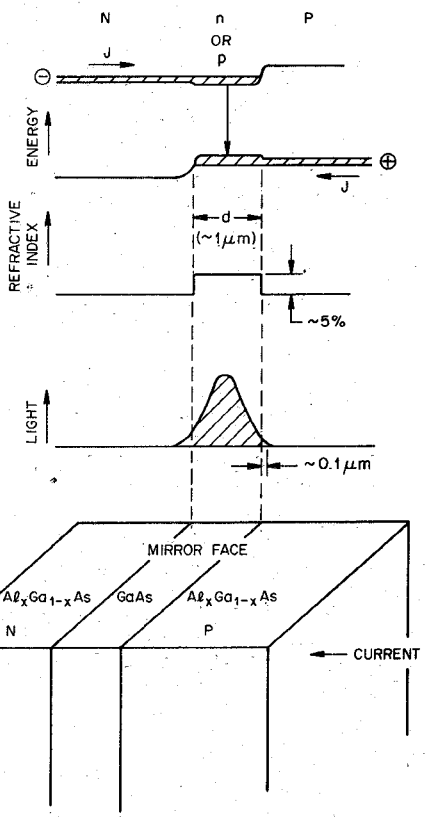

Fig. 10. Schematic representation of the band edges with forward bias, refractive index changes, optical-field distribution, and physical structure of a DH laser diode. After Panish and Hayashi [21].

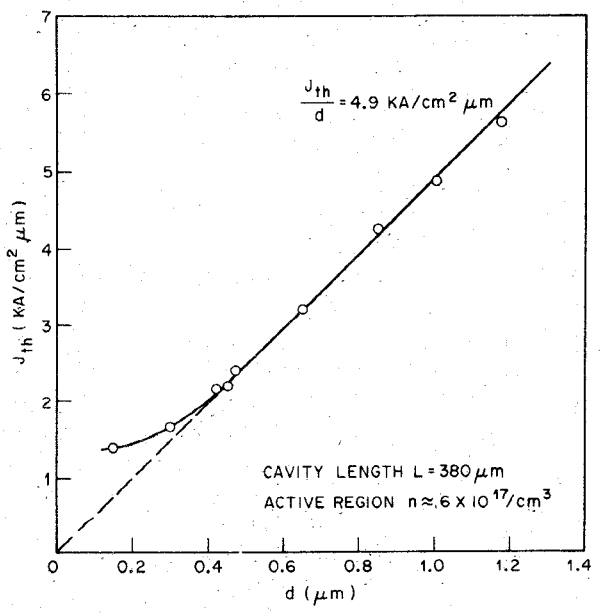

Fig. 11. Threshold current as a function of d at room temperature for a series of similarly doped "uniform" DH lasers. Cavity length is 380 μm; active region $n = 6 \times 10^{17}/cm^3$. After Pinkas *et al.* [68].

lasers described in the following provide several methods for transverse-mode control. It should be noted here that because of the weaker optical confinement of homostructure and SH lasers, these lasers usually operate in the fundamental transverse mode without further modification.

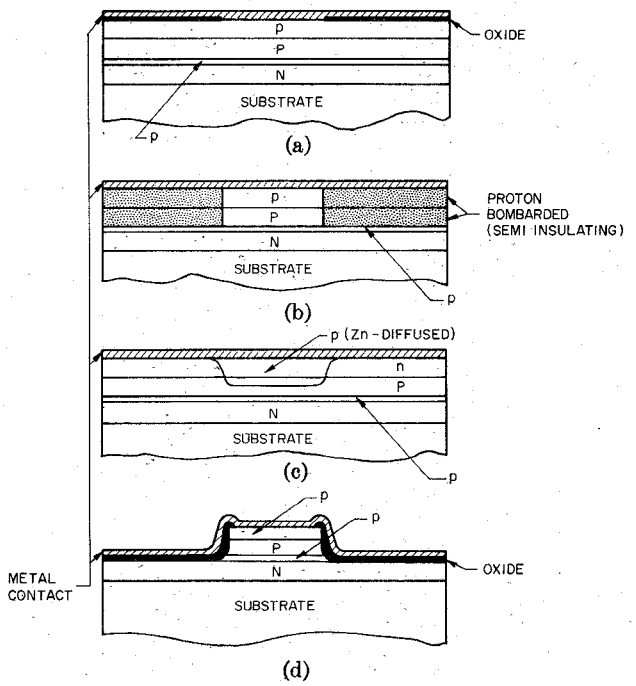

Fig. 12. End (mirror) view of four types of stripe-contact lasers. (a) Stripe contact. (b) Proton-bombardment defined stripe. (c) Doping-profile stripe control. (d) Stripe mesa.

At this point it is useful to consider the optical-field distribution within the structure and in the far field of a DH laser. The laser emission is strongly divergent because of the small size of the source. This divergence is particularly great perpendicular to the junction plane because the source dimensions there are near or less than the lasing wavelength within the structure. The optical-field intensity distribution (E^2) for the fundamental mode perpendicular to the junction plane within the structure is shown for a set of structures with different active-region widths but the same wide-gap Al compositions [48] in Fig. 13. It is interesting to note that for sufficiently narrow structures ($d < \lambda/2$) the field cannot be as effectively confined and spreads rapidly beyond the active region with decreasing d. The effect of the active-layer thickness and the ternary composition upon the far-field distribution of the fundamental mode is clearly seen in Fig. 14. For very small d the effective dimension of the source becomes larger and with decreasing d the divergence perpendicular to the plane of the junction becomes smaller. Unfortunately, the pumped region d is then an increasingly smaller part of the distribution and eventually the lasing-threshold current density must increase with decreasing d. It is also clear that the fundamental transverse-mode operation is restricted to DH lasers with active regions less than about 0.7 μm since the cavity width can support higher order transverse modes at larger d. The far-field intensity distribution for a typical DH laser emitting in the fundamental transverse and parallel modes is shown in Fig. 15. For comparison the far-field intensity distribution perpendicular to the junction plane for a DH laser with a second-order mode is shown as the dashed

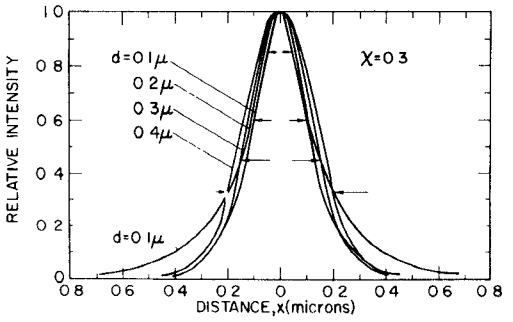

Fig. 13. The square of the electric field as a function of position within a GaAs–$Al_xGa_{1-x}As$ DH laser. The distance is measured from the center of the active region in the direction normal to the plane of the junction. Al concentration is $x = 0.3$. The arrows indicate the active region width d for each curve. After Casey *et al.* [48].

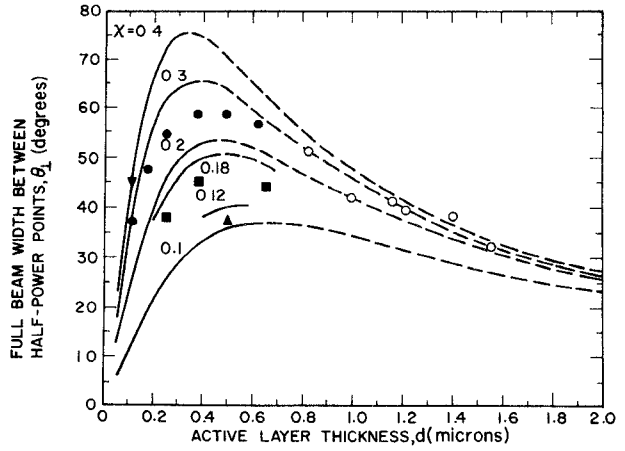

Fig. 14. Full beamwidth at the half-power (3-dB) points as a function of active layer thickness d and composition x for the DH. The solid and dashed curve is the beam divergence calculated for the fundamental TE mode. The dashed portion of the calculated curve represents active-layer thicknesses where higher order modes are possible. The open circles are for SCH lasers (fundamental mode). Data and calculations from [48] and [55].

curve in Fig. 16. (The zero-order mode also shown in Fig. 16 is for an SCH laser described in the following.)

Not only do the dielectric steps parallel to the junctions, but also the mirror ends act as sources of standing waves. Between these mirrors sets of standing waves constitute the longitudinal modes. These, as all other modes, are separated in frequency. It can be shown that because the gain profile of injection lasers is very wide, about 200 Å, and because the typical laser diode length is about 500 μm, the optical cavity supports many longitudinal modes separated by about 1–3 Å with only slightly differing gain. As illustrated in Fig. 17, many modes may lase simultaneously. A single longitudinal mode is much more difficult to obtain than a single transverse or parallel mode. Rossi *et al.* [49] have achieved single longitudinal-mode operation by coupling an external grating to a homostructure and a SH laser, respectively. The situation should be similar for DH and SCH lasers described in the following but it is doubtful whether an external cavity for mode control will be practical for other than laboratory use.

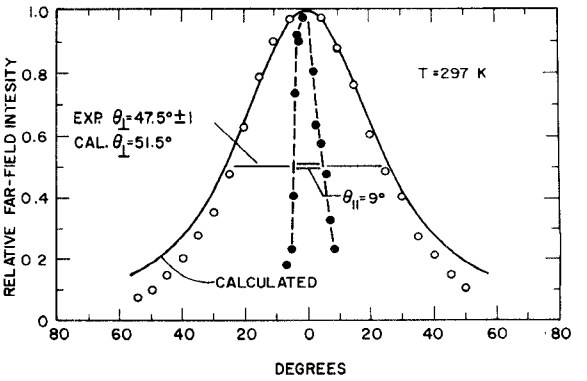

Fig. 15. Far-field pattern for a DH laser with $d = 0.18$ μm and $x = 0.3$. The experimental intensity in the plane of the junction is given by the solid dots ●, and the angle at half intensity is shown by $\theta_{||}$. The experimental intensity perpendicular to the junction plane is given by the open dots ○, and the calculated intensity is shown by the solid line. After Casey *et al.* [48].

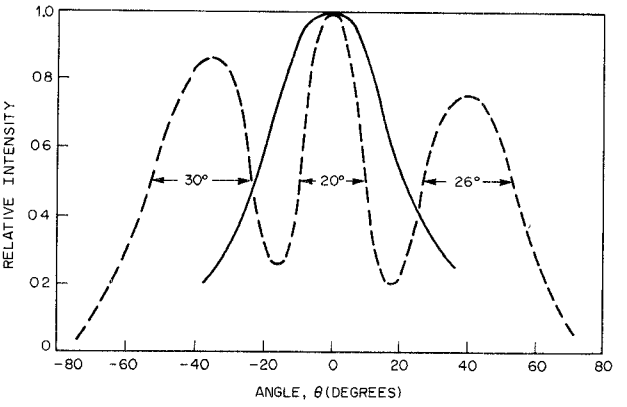

Fig. 16. Far-field intensity distribution perpendicular to the junction for an SCH laser—and a DH laser---both with an optical cavity width of 1.05 μm and an Al concentration of $x = 0.3$ in the wide-gap regions. Curves replotted from [55]

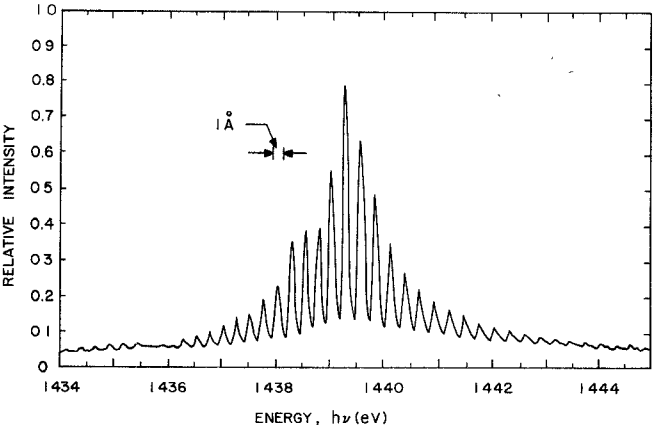

Fig. 17. Lasing spectrum of a single transverse-mode DH laser with multiple longitudinal modes.

D. *Separate-Confinement Heterostructure Lasers*

Several types of structures in which the carriers are confined to a region narrower than the waveguide have been studied. All of these may be classified as SCH lasers although they fall into two somewhat different subclassifications. The simplest of these (N-n-p-P) uses a p–n

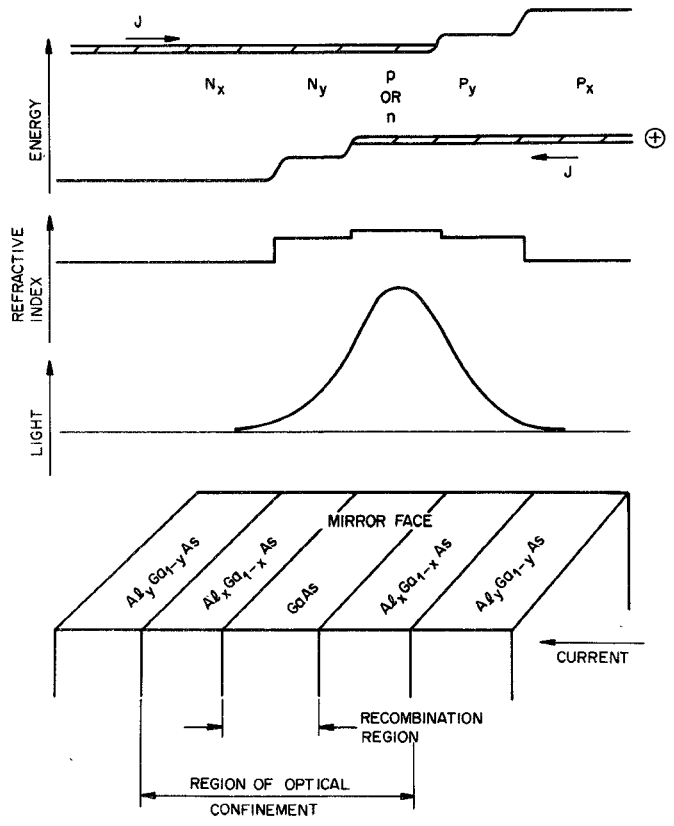

Fig. 18. Schematic representation of the band edges with forward bias, refractive-index changes, optical-field distribution, and physical structure of a symmetrical SCH laser. After Panish and Hayashi [21].

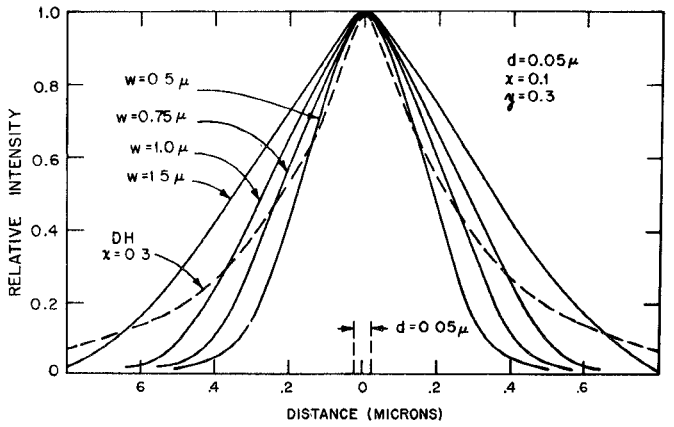

Fig. 19. Square of the electric field as a function of position within SCH and DH lasers with the electrically active region width of both equal to 0.05 μm but at several optical cavity widths for the SCH. After Casey *et al.* [55].

junction within the active region so that as a result of the preference for electron injection in GaAs the gain is limited to only a portion of the active region. The large-optical-cavity (LOC) laser described by Kressel *et al.* [50], [51] is typical of this class. This structure was intended to yield high-power pulsed lasers as a result of its greater efficiency while maintaining a relatively large cavity width to reduce optical-power density. The same structure with the p-n junction properly placed within the optical cavity (a ratio of thickness of the p and n regions of 2:1) may be used to maintain a fundamental transverse mode for a relatively wide waveguide at currents well above threshold [52].

A somewhat more complex structure based upon suggestions by Hayashi [53] and Thompson and Kirkby [54] has also been studied. These authors pointed out that carriers are more easily confined than light by small changes in the band gap at the heterojunction and that the gain in heterostructure lasers depends superlinearly upon current. They suggested that it should be possible to separately confine the carriers to a small fraction of the total optical cavity w while achieving sufficient gain to permit the threshold to decrease as the electrically active layer thickness d decreases.

The notation used previously may be extended to these structures with minor modification. They may be designated N_x-N_y-p-P_y-P_x or N_x-N_y-n-P_y-P_x. Here x and y denote the Al composition in the layers $Al_xGa_{1-x}As$ or $Al_yGa_{1-y}As$ and $x > y$. A typical structure is illustrated in Fig. 18, and a typical set of the optical electric-field distributions for the fundamental mode within the structure for several SCH lasers with different w is compared with a DH laser in Fig. 19. This illustrates that for very narrow electrically active regions the SCH confines the fundamental mode better than the DH, and also that the coupling of the gain region to the fundamental mode is better. In addition, in the symmetrical SCH illustrated in Fig. 18, the fundamental transverse mode is pumped preferentially to all other transverse modes and that mode persists to wide optical-region widths. This is shown for measurements of the half-power beamwidth for several SCH lasers (the open circles) in Fig. 14 and as the solid curve of Fig. 16. The result of the better coupling of the gain to the fundamental mode in SCH lasers than in DH lasers is, as is shown in Table I, that the lowest current-density thresholds have been obtained in these lasers. Furthermore, as is also shown in Table I, the SCH lasers also have somewhat higher efficiencies than DH lasers. The reason for the higher efficiencies is not clear but it has been speculated [55] that this may result from less scatter and less spreading of the optical field out of the structure in SCH lasers. Some typical parameters for SCH lasers are given in Tables I and II.

DEGRADATION OF HETEROSTRUCTURE LASERS

The degradation of injection lasers is a subject which has been characterized by confusion and conflicting information. It is not possible in this brief review to consider all of the earlier experiments and theories. A great deal of progress has been made in the last 18 months or so, and when considering gradual degradation only recent studies will be considered. Degradation during very high pulsed-current operation occurs by a so-called "catastrophic" mode. It is characterized by gross damage (melting, cracking) of the structure. This degradation is apparently related to a power-density limit at the mirrors of 10^6–10^7 W/cm^2. Thus lasers with thin optical

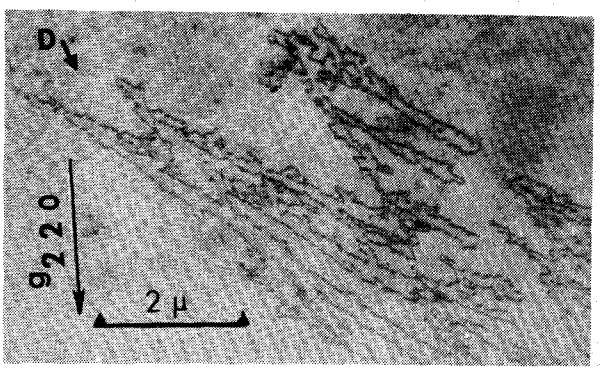

Fig. 20. Bright-field electron micrograph showing a dislocation (*D*) which is at the origin of a dislocation network forming a DLD. After Petroff and Hartman [59].

cavities, such as very low-threshold DH lasers, fail catastrophically at lower pulsed power than do lasers with wide optical cavities or lasers in which the field may spread out of the active region (as with homostructure or SH lasers). Thus lasers intended for high pulsed-power operation have generally been homostructure or SH lasers and low-threshold current is sacrificed for high power at the catastrophic degradation limit. It is worth mentioning here, however, that with the SCH lasers it is possible to make a much better compromise so that relatively low thresholds and relatively high-power thresholds for catastrophic degradation may be achieved with the same laser. A review of catastrophic failure has been given by Kressel [56].

Since lasers used for optical communications will in general be operated as modulated CW devices, we are not primarily concerned with catastrophic degradation, but rather with the second type of degradation—the so-called gradual degradation of injection lasers. In the past year or so an impressive amount of progress has been made towards the understanding and control of gradual degradation. The first DH lasers degraded in a matter of minutes or hours under CW operation to the point at which CW lasing could not be sustained. This rapid degradation was characterized [57], [58] by the appearance of nonluminescent areas called dark-line defects (DLD) crossing the active regions of the lasers during lasing. The DLD has been identified with transmission electron microscopy by Petroff and Hartman [59] as a three-dimensional dislocation network which originates at a dislocation crossing the $Al_xGa_{1-x}As$ and GaAs epitaxial layers. The latter is clearly seen in Fig. 20. The three-dimensional properties of the network have been observed with stereo-pair photographs. The DLD apparently grows by a climb mechanism during operation of the laser. The source of the point defects required for DLD growth and their driving force are not presently understood. Hartman and Hartman [58] have shown that the lasing lifetime is strongly related to strain, and reduced-strain electrical contacts permitted an increase in laser lifetime from tens of hours to several thousand hours at 20°C [60] and at 30°C [61] ambient temperature. The DLD's are generally not present in operating long-lived lasers.

It has also been established [62], [63] that LPE layers of $Al_xGa_{1-x}As$ on GaAs are compressively stressed at room temperature to levels of 10^8–10^9 dyn cm^{-2} depending on x. This elastic stress can be accounted for by differences in the thermal expansion coefficients of GaAs and $Al_xGa_{1-x}As$ which have the same lattice parameter near the growth temperature. It has been speculated that this stress in heterostructure layers also leads to gradual degradation of DH lasers. Such stress may be removed [64] from the laser structures by the use of $Al_xGa_{1-x}P_yAs_{1-y}$ with $y \approx 0.015$ for the wide band-gap region of the laser. Since P is isoelectronic with As, the small amount present in the quaternary does not materially affect the device electrically or optically, but the relatively small covalent radius of P permits correction of the lattice parameters so that they match at room temperature.

Many DH lasers with GaAs–$Al_xGa_{1-x}P_yAs_{1-y}$ heterojunctions have been studied during CW lasing operations at elevated temperatures [41]. Stable operations with lifetimes greater than 10^5 h are predicted for these lasers when the data are extrapolated to room temperature. Furthermore, these lasers have somewhat lower room-temperature current thresholds [65] than do GaAs–$Al_xGa_{1-x}As$ DH lasers. Although it is believed that the reduced strain is related to both the increased lifetime and reduced threshold of the lasers with the quaternary wide-gap regions, the mechanism by which this occurs is not known.

CONCLUSION

The past few years have been a period of intensive activity in the study of heterostructure lasers. Continuous lasing and vastly reduced room-temperature current thresholds have resulted from the recognition that both optical and carrier confinement can be achieved by utilizing the lattice-matching and band-edge properties at the GaAs–$Al_xGa_{1-x}As$ heterojunction. Detailed studies of the physical and chemical properties have led to the capability for the growth of complex structures and the understanding of the behavior of these structures as lasers. Modification of the composition of the wide-gap region and the development of strain-free fabrication procedures have led to very long-lived lasers. The result of all of this is that the heterostructure laser is a prime candidate to be the optical source in optical-communications systems.

REFERENCES

[1] N. G. Basov, O. N. Krokhin, and Y. M. Popov, *Pis'ma Zh. Eksp. Teor. Fiz.*, vol. 40, p. 1879, 1961; also *Sov. Phys.—JETP*, vol 13, p. 1320, 1961.
[2] M. G. A. Bernard and G. Duraffourg, *Phys. Status Solidi*, vol. 1, p. 699, 1961.
[3] R. N. Hall, G. E. Fenner, J. D. Kingsley, T. J. Soltys, and R. O. Carlson, *Phys. Rev. Lett.*, vol. 9, p. 366, 1962.
[4] M. I. Nathan, W. P. Dumke, G. Burns, F. H. Dill, and G. J. Lasher, *Appl. Phys. Lett.*, vol. 1, p. 62, 1962.
[5] T. M. Quist *et al.*, *Appl. Phys. Lett.*, vol. 1, p. 91, 1962.
[6] N. Holonyak, Jr., and S. F. Beracqa, *Appl. Phys. Lett.*, vol. 1, p. 82, 1962.
[7] H. Kroemer, "A proposed class of heterojunction injection lasers," *Proc. IEEE* (Corresp.), vol. 51, pp. 1782–1783, Dec. 1963.

[8] Zh. I. Alferov and R. F. Kazarinov, Author's certificate 1032155/26-25, USSR, 1963 (as cited in Alferov *et al.* [9]).
[9] Zh. I. Alferov *et al.*, *Fiz. Tverd. Tela*, vol. 9, p. 279, 1967; also *Sov. Phys.—Solid State*, vol. 9, p. 208, 1967.
[10] Zh. I. Alferov, *Fiz. Tekh. Poluprov.*, vol. 1, p. 436, 1967; also *Sov. Phys.—Semicond.*, vol. 1, p. 358, 1967.
[11] H. Rupprecht, J. M. Woodall, and D. G. Pettit, *Appl. Phys. Lett.*, vol. 11, p. 81, 1967.
[12] H. C. Casey, Jr., and M. B. Panish, *J. Appl. Phys.*, vol. 40, p. 4910, 1969.
[13] Zh. I. Alferov, V. M. Andreev, V. I. Korol'kov, E. L. Portnoi, and D. N. Tret'yakov, *Fiz. Tekh. Popuprov.*, vol. 2, p. 1016, 1968; also *Sov. Phys.—Semicond.*, vol. 2, p. 843, 1969.
[14] ——, in *Proc. 9th Int. Conf. Physics of Semiconductors* (1968), p. 504.
[15] I. Hayashi, M. B. Panish, and P. W. Foy, "A low-threshold room-temperature injection laser," *IEEE J. Quantum Electron.* (Corresp.), vol. QE-5, pp. 211–212, Apr. 1969.
[16] M. B. Panish, I. Hayashi, and S. Sumski, "A technique for the preparation of low-threshold room-temperature GaAs laser diode structures," *IEEE J. Quantum Electron.* (Corresp.), vol. QE-5, pp. 210–211, Apr. 1969.
[17] I. Hayashi and M. B. Panish, *J. Appl. Phys.*, vol. 41, p. 150, 1970.
[18] H. Kressel and H. Nelson, *RCA Rev.*, vol. 30, p. 106, 1969.
[19] I. Hayashi, M. B. Panish, P. W. Foy, and S. Sumski, *Appl. Phys. Lett.*, vol. 17, p. 109, 1970.
[20] Zh. I. Alferov *et al.*, *Fiz. Tekh. Poluprov.*, vol. 4, p. 1826, 1970.
[21] M. B. Panish and I. Hayashi, *Applied Solid State Sciences*, vol. 4, R. Wolfe, Ed. New York: Academic, 1974, pp. 235–328.
[22] M. B. Panish and S. Sumski, *Phys. Chem. Solids*, vol. 30, p. 129, 1969.
[23] M. Ilegems and G. L. Pearson, in *1968 Proc. Symp. Gallium Arsenide* (1969), p. 3.
[24] A. Onton, M. R. Lorenz, and J. M. Woodall, *Bull. Amer. Phys. Soc.*, vol. 16, p. 371, 1971.
[25] O. Berolo and J. C. Woolley, *Can. J. Phys.*, vol. 49, p. 1335, 1971.
[26] H. C. Casey, Jr., E. Pinkas, and B. I. Miller, *J. Appl. Phys.*, vol. 44, p. 1281, 1973.
[27] H. Schade, H. Nelson, and H. Kressel, *Appl. Phys. Lett.*, vol. 18, p. 121, 1971.
[28] Zh. I. Alferov, V. M. Andreev, V. I. Morgyin and V. I. Stremin, *Sov. Phys.—Semicond.*, vol. 3, p. 1234, 1970; also *Fiz. Tekh. Poluprov.*, vol. 3, p. 1470 1969.
[29] D. D. Sell, H. C. Casey, Jr., and K. Wecht, *J. Appl. Phys.*, vol. 45, p. 2650, 1974.
[30] H. C. Casey, Jr., D. D. Sell, and M. B. Panish, *Appl. Phys. Lett.*, vol. 24, p. 63, 1974.
[31] A. Y. Cho *et al.*, *Appl. Phys. Lett.*, vol. 25, p. 288, 1974.
[32] Zh. I. Alferov, V. M. Andreev, S. G. Konnikov, V. G. Nitkin, and D. N. Tret'yakov, in *Proc. Int. Conf. Heterojunctions I* (1971), p. 93.
[33] W. G. Rado, W. J. Johnson, and L. I. Crawley, *J. Electrochem. Soc.*, vol. 119, p. 652, 1972.
[34] M. B. Panish and M. Ilegems, *Progress in Solid State Chemistry*, vol. 7, H. Reiss and W. O. McCaldin, Ed. New York: Pergamon, 1972, pp. 39–83.
[35] J. R. Arthur, *J. Appl. Phys.*, vol. 39, p. 4032, 1968.
[36] A. Y. Cho, M. B. Panish, and I. Hayashi, in *Proc. Symp. Gallium Arsenide and Related Compounds* (Aachen, Germany, 1970), p. 18.
[37] A. Y. Cho, *J. Vac. Sci. Technol.*, vol. 8, p. 531, 1971.
[38] J. Womac and R. H. Rediker, *J. Appl. Phys.*, vol. 43, p. 4148, 1972.
[39] Zh. I. Alferov *et al.*, *Fiz. Tekh. Poluprov.*, vol. 5, p. 972, 1971; also *Sov. Phys.—Semicond.*, vol. 5, p. 858, 1971.
[40] a) J. C. Dyment, L. A. D'Asaro, J. C. North, B. I. Miller, and J. E. Ripper, "Proton-bombardment formation of stripe-geometry heterostructure lasers for 300 K CW operation," *Proc. IEEE* (Lett.), vol. 60, pp. 726–728, June 1972.
b) J. C. Dyment, L. A. D'Asaro, and J. C. North, *Bull. Amer. Phys. Soc.*, vol. 16, p. 329, 1971.
[41] R. L. Hartman, private communication.
[42] J. E. Ripper, J. C. Dyment, L. A. D'Asaro, and T. L. Paoli, *Appl. Phys. Lett.*, vol. 18, p. 155, 1971.
[43] H. Yonezu *et al.*, *Japan. J. Appl. Phys.*, vol. 12, p. 1585, 1973.
[44] T. Tsukada, R. Ito, H. Nakashima, and O. Nakada, "Mesa-stripe-geometry double-heterostructure injection lasers," *IEEE J. Quantum Electron.*, (*Special Issue on 1972 IEEE Semiconductor Laser Conference*), vol. QE-9, pp. 356–361, Feb. 1973.
[45] L. A. D'Asaro, *J. Luminescence*, vol. 7, p. 310, 1973.
[46] W. O. Schlosser, *Bell Syst. Tech. J.*, vol. 52, p. 887, 1973.
[47] F. R. Nash, *J. Appl. Phys.*, vol. 44, p. 4696, 1973.
[48] H. C. Casey, Jr., M. B. Panish, and J. L. Merz, *J. Appl. Phys.*, vol. 44, p. 5470, 1973.
[49] J. A. Rossi, S. R. Chinn, and H. Heckscher, *Appl. Phys. Lett.*, vol. 23, p. 25, 1973.
[50] H. F. Lockwood, H. Kressel, H. S. Sommers, and F. Z. Hawrylo, *Appl. Phys. Lett.*, vol. 17, p. 499, 1970.
[51] H. Kressel, H. F. Lockwood, and F. Z. Hawrylo, *Appl. Phys. Lett.*, vol. 18, p. 43, 1971.
[52] T. L. Paoli, B. W. Hakki, and B. I. Miller, *J. Appl. Phys.*, vol. 44, p. 1276, 1973.
[53] I. Hayashi, U. S. Patent 3 691 476, 1972.
[54] G. H. B. Thompson and P. A. Kirkby, "(GaAl)As lasers with a heterostructure for optical confinement and additional heterojunctions for extreme carrier confinement," *IEEE J. Quantum Electron.* (*Special Issue on 1972 IEEE Semiconductor Laser Conference*), vol. QE-9, pp. 311–318, Feb. 1973.
[55] H. C. Casey, Jr., M. B. Panish, W. O. Schlosser, and T. L. Paoli, *J. Appl. Phys.*, vol. 45, p. 322, 1974.
[56] H. Kressel, *Lasers*, vol. 3, A. K. Levine and A. D. Maria, Ed. New York: Marcel Dekka, 1971, p. 49.
[57] B. C. DeLoach, Jr., B. W. Hakki, R. L. Hartman, and L. A. D'Asaro, "Degradation of CW GaAs double-heterojunction lasers at 300 K," *Proc. IEEE* (Lett.), vol. 61, pp. 1042–1044, July 1973.
[58] R. L. Hartman and A. R. Hartman, *Appl. Phys. Lett.*, vol. 23, p. 147, 1973.
[59] P. Petroff and R. L. Hartman, *Appl. Phys. Lett.*, vol. 23, p. 469, 1973.
[60] H. Yonezu *et al.*, presented at the Conf. Solid State Devices, Tokyo, Japan, 1973.
[61] R. L. Hartman, J. C. Dyment, C. J. Hwang, and M. Kuka, *Appl. Phys. Lett.*, vol. 23, pp. 181 and 491, 1973.
[62] G. A. Rozgonyi, C. J. Hwang, and T. J. Ciesielka, *J. Electrochem. Soc.*, vol. 120, p. 333C, 1973.
[63] F. K. Reinhart and R. A. Logan, *J. Appl. Phys.*, vol. 44, p. 3173, 1973.
[64] G. A. Rozgonyi and M. B. Panish, *Appl. Phys. Lett.*, vol. 23, p. 533, 1973.
[65] J. C. Dyment *et al.*, *Appl. Phys. Lett.*, vol. 24, p. 481, 1974.
[66] H. Kressel, H. Nelson, and F. Z. Hawrylo, *J. Appl. Phys.* vol. 41, p. 2019, 1970.
[67] E. Pinkas, B. I. Miller, I. Hayashi, and P. W. Foy, "Additional data on the effect of doping on the lasing characteristics of GaAs–$Al_xGa_{1-x}As$ double-heterostructure lasers," *IEEE J. Quantum Electron.* (*Special Issue on 1972 IEEE Semiconductor Laser Conference*), vol. QE-9, pp. 281–282, Feb. 1973.
[68] ——, *J. Appl. Phys.*, vol. 43, p. 2827, 1972.
[69] G. H. B. Thompson and P. A. Kirkby, *Electron. Lett.*, vol. 9, p. 295, 1973.
[70] B. I. Miller, E. Pinkas, I. Hayashi, and R. J. Capik, *J. Appl. Phys.*, vol. 43, p. 2817, 1972.
[71] L. R. Dawson, to be published.
[72] D. Rode, *J. Growth Cryst.*, vol. 20, p. 13, 1973.
[73] B. W. Hakki and C. J. Hwang, *J. Appl. Phys.*, vol. 45, p. 2168, 1974.